








Spontaneous Article

The first and most complete dinosaur skeleton from the Middle Jurassic of Scotland

Elsa PANCIROLI^{1*} , Gregory F. FUNSTON² ,
Susannah C. R. MAIDMENT^{3,4} , Richard J. BUTLER⁴ ,
Roger B. J. BENSON⁵ , Brett L. CRAWFORD^{6†}, Matt FAIR⁶,
Nicholas C. FRASER¹  and Stig WALSH¹ 

¹ Geography, Earth & Environmental Sciences, National Museums Scotland, Edinburgh, Scotland, EH1 1JF, UK.

² Department of Earth and Planetary Sciences, University of California, Davis, CA, USA.

³ Reptiles, Amphibians and Birds Section, The Natural History Museum, Cromwell Road, London, SW7 5BD, UK.

⁴ School of Geography, Earth & Environmental Sciences, University of Birmingham, Birmingham, B15 2TT, UK.

⁵ American Museum of Natural History, New York, NY, USA.

⁶ Research Casting International, 15 Dufferin Avenue, Trenton, ON, K8V 5C8, Canada.

*Corresponding author E-mail: e.panciroli@nms.ac.uk

ABSTRACT: The fossil record of dinosaurs in Scotland mostly comprises isolated highly fragmentary bones from the Great Estuarine Group in the Inner Hebrides (Bajocian–Bathonian). Here we report the first definite dinosaur body fossil ever found in Scotland (historically), having been discovered in 1973, but not collected until 45 years later. It is the first and most complete partial dinosaur skeleton currently known from Scotland. NMS G.2023.19.1 was recovered from a challenging foreshore location in the Isle of Skye, and transported to harbour in a semi-rigid inflatable boat towed by a motor boat. After manual preparation, micro-CT scanning was carried out, but this did not aid in identification. Among many unidentifiable elements, a neural arch, two ribs and part of the ilium are described herein, and their features indicate that this was a cerapodan or ornithopod dinosaur. Histological thin sections of one of the ribs support this identification, indicating an individual at least eight years of age, growing slowly at the time of death. If ornithopodan, as our data suggest, it could represent the world's oldest body fossil of this clade.



KEY WORDS: Bathonian, histology, Kilmaluag Formation, Ornithischia.

Introduction

Dinosaurs from the Triassic and Early Jurassic were generally small, bipedal carnivores and omnivores, but by the Late Jurassic they had radiated into a highly diverse range of species that included some of the largest terrestrial vertebrates to ever walk the Earth (Brusatte *et al.* 2010). This major diversification and radiation of dinosaurs appears to have primarily occurred during the Middle Jurassic (Butler *et al.* 2008; Maidment *et al.* 2020, 2021; Wills *et al.* 2021, 2023), making dinosaurs from this time interval critical to our understanding of the drivers of this radiation. However, Middle Jurassic dinosaur fossils are exceptionally poorly known and globally rare (Benson *et al.* 2016; Maidment *et al.* 2020). Consequently, the early evolutionary histories and major diversifications of most dinosaur groups remain obscure. New dinosaur finds from the Middle Jurassic are therefore highly significant for our understanding of the development of dinosaur-dominated ecosystems.

Fossiliferous Middle Jurassic deposits from Scotland have provided exceptionally well-preserved skeletons of small vertebrates,

including stem lizards (Tałanda *et al.* 2022), salamanders (Jones *et al.* 2022) and mammaliaforms (Panciroli *et al.* 2021, 2022, 2024), but the dinosaur fossil record is scant. The moderately complete but very poorly preserved postcranial skeleton of *Saltopus elginensis*, from the Late Triassic deposits of Elgin (Huene 1910; Benton & Walker 2011) has most commonly been considered an early dinosauriform, closely related to, but outside Dinosauria (Benton & Walker 2011). Although some analyses have tentatively placed it within Dinosauria (e.g. Baron *et al.* 2017), given the preservation of this specimen we consider its phylogenetic position uncertain. Definite dinosaur body fossils from the Middle Jurassic are geographically confined to the Isles of Skye and Eigg (Whyte & Ross 2019). The first specimens to be described from a Scottish locality were an indeterminate sauro-pod limb bone from the Bathonian of Trotternish (Clark *et al.* 1995) and an incomplete theropod tibia, first described in 1995 but recently compared to *Sarcosaurus woodi* (Ezcurra *et al.* 2023) from the Sinemurian of Strathaird, Skye.

Since the 1990s, only isolated and incomplete body fossils have been described from the Bathonian Lealt Shale, Valtos and Kilmaluag Formations, and the older (Aalenian to Bajocian) Bear-raig Sandstone Formation (Aalenian to Bajocian) and

†Brett Lloyd Crawford, 1974–2023.

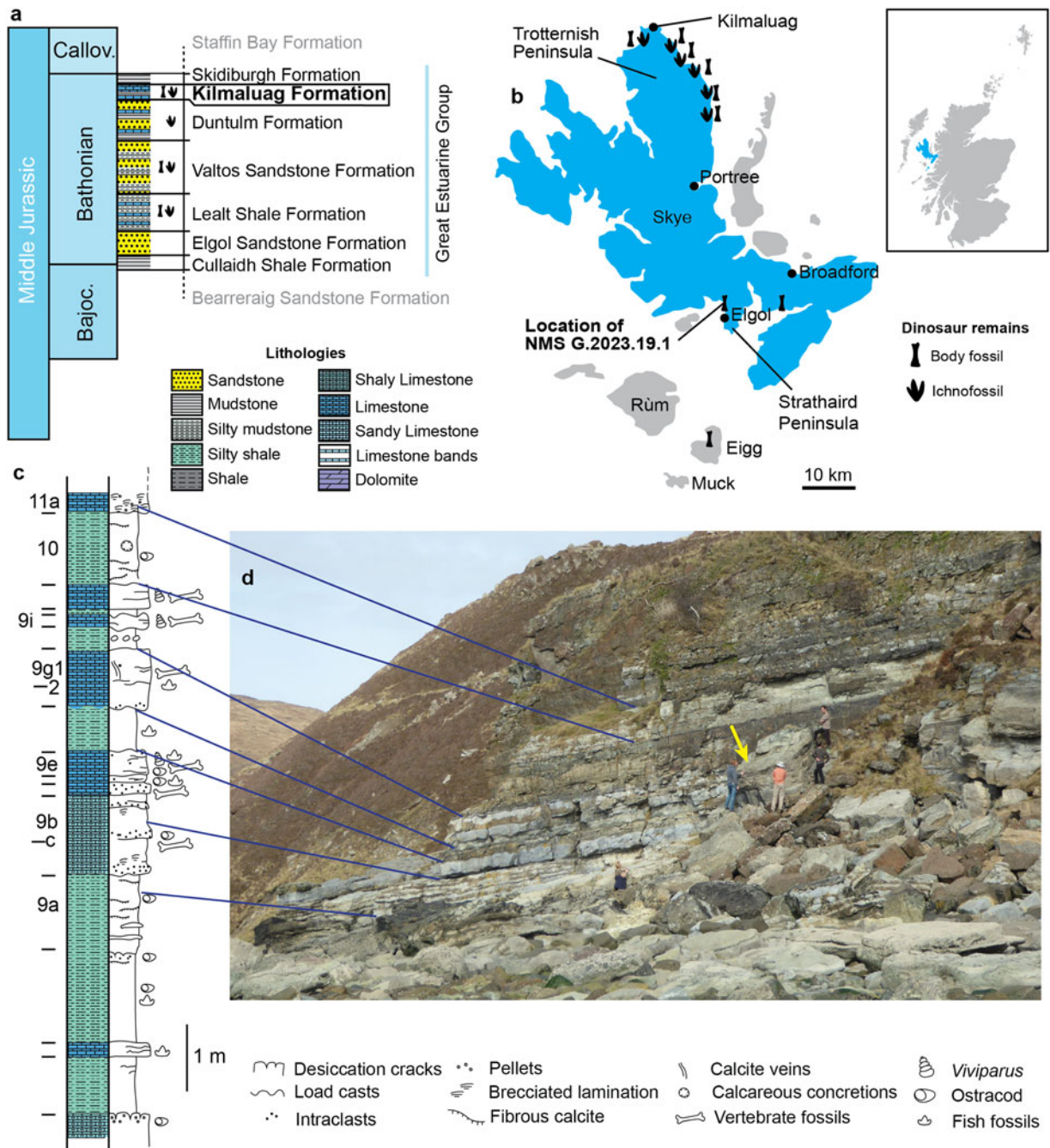


Figure 1 Location and geological context of discovery of NMS G.2023.19.1: (a) stratigraphic column showing the Great Estuarine Group and Kilmaluag Formation, and presence of dinosaur body and trace fossils; (b) locations of Skye and Eigg, where dinosaur fossils have been found, and location of NMS G.2023.19.1; (c) stratigraphic column of the Carn Mor landslip, adapted from Panciroli *et al.* (2020b); (d) position of NMS G.2023.19.1 on the foreshore in 2017, with stratigraphic column matched with (c). Team in (d) left to right: Richard Butler, Roger Benson, Rubén Contreras Izquierdo, Stig Walsh. Photograph by E. Panciroli.

Broadford Beds Formation (Sinemurian) (Fig. 1a, b). These include individual teeth and bones of sauropod (Barrett 2006; Clark & Gavin 2016) and theropod (Brusatte & Clark 2015; Young *et al.* 2019) dinosaurs, and the ulna and radius of a thyreophoran (Clark 2001; Panciroli *et al.* 2020a). The dinosaur ichnofossil record on Skye includes single prints and multiple trackways from the Bathonian Lealt Shale, Valtos, Duntulm and Kilmaluag formations (for an overview see Clark 2018a). These include tracks attributed to ornithischians, theropods and sauropods. Potential dinosaur trackways have also been informally reported from the east coast of mainland Scotland, from Keiss (Panciroli & Walsh unpublished data) and an undisclosed site north of Inverness (Clark 2018b). Whyte & Ross (2019) provide an accessible overview of most vertebrate fossil discoveries on Skye.

The Bathonian Kilmaluag Formation has yielded a small number of dinosaur ichnological and body fossils on the Isle of Skye, representing the geologically youngest non-avian dinosaur material in Scotland. Small tridactyl trackways are known from the Kilmaluag outcrops on the Trotternish Peninsula in north-east Skye (Clark *et al.* 2005). On the Strathaird Peninsula in southern Skye, dinosaur body fossil remains reported to date comprise an isolated sauropod tooth, potentially attributable to a basal eusauropod or basal titanosauriform (Barrett 2006), and an incomplete taxonomically indeterminate femur and theropod tooth (Wills *et al.* 2014).

Here we describe the partial skeleton of a dinosaur from the Kilmaluag Formation in Skye. It comprises the most complete fossil of its kind in Scotland, and its original discovery pre-dates the first reported dinosaur fossils from Skye. Although

incomplete, comparative anatomy and histological analysis allow us to narrow the identification of the specimen. Its extraction was logistically challenging, and so we also outline the method of collection from the dynamic coastline of the island.

Institutional abbreviations: NMS = National Museums Scotland, Edinburgh; NHMUK = Natural History Museum, London.

1. History of discovery of NMS G.2023.19.1

Abundant invertebrate fossils were described by early geologists working in the Isle of Skye in the 19th Century (e.g., Murchison 1828), and some vertebrate fossil fragments are mentioned in early descriptions of the local geology (Peach 1910; Arkell 1933). However, collection of vertebrate fossils from the Kilmaluag Formation did not begin until 1971, when the significance of these beds was recognised by Dr Michael Waldman, a palaeontologist and teacher leading a Duke of Edinburgh's Award group from Stowe School (Waldman & Savage 1972).

Waldman and Professor Robert Savage of the University of Bristol subsequently led seven field trips to Skye and surrounding parts of the Inner Hebrides between 1971 and 1982. Savage recorded the discovery of a large vertebrate fossil in his field notebook on 21 May 1973. His sketch of the specimen (Fig. 2) matches the fossil subsequently rediscovered in 2015 and described here (NMS G.2023.19.1).

Savage noted it as 'Bones of ?Dinosaur on big block, v large prob [*sic*] land reptile'. However, there is no further mention of the specimen nor of any attempts to extract it in Savage's field notebook. This may have been due to the size and position of the specimen on the foreshore, or because its significance was not recognised at the time.

Almost 20 years later, a partial limb bone of a sauropod dinosaur was found in the Valtos Sandstone Formation near Valtos (Clark *et al.* 1995) and shortly afterwards a partial theropod tibia was found in the Broadford Beds Formation at Heaste (Benton *et al.* 1995; Ezcurra *et al.* 2023). Until now, these were thought to be the first dinosaur body fossils found in Scotland.

NMS G.2023.19.1 was rediscovered in 2015 by SW and RJB during fieldwork at the locality, but was considered too difficult to collect at that time. In 2017 the situation was re-evaluated, and extraction was led by EP the following year.

2. Geological background

NMS G.2023.19.1 was found in exposures of the Kilmaluag Formation north of the village of Elgol on the Isle of Skye, at the site known in the literature as 'S. Carn Mor' (e.g., Andrews 1985). The Kilmaluag Formation is part of the Great Estuarine

Group, a series of near-shore shallow marine, brackish and fresh-water lagoon sediments of Bathonian age (Judd 1878; Harris & Hudson 1980; Andrews 1985; Barron *et al.* 2012). The Kilmaluag Formation was named for the village of Kilmaluag on the northern tip of the Isle of Skye, where the type section is located (Harris & Hudson 1980). However, it crops out in multiple locations on Skye and the neighbouring Inner Hebridean islands of Eigg and Muck, with the thickest sections (about 25 m) located on the Strathaird Peninsula on Skye (Harris & Hudson 1980; Morton & Hudson 1995).

The Kilmaluag Formation is correlated with the Retrocostatum Zone, of late Bathonian age, ~166.1 Ma (Barron *et al.* 2012; Cohen *et al.* 2019). It represents freshwater facies and is defined by the occurrence of ostracod-bearing calcareous mudstones and marls/fissile mudstones which earned it the former name of 'Ostracod Limestone' (Anderson & Dunham 1966; Harris & Hudson 1980; Andrews 1985; Barron *et al.* 2012).

A diverse vertebrate faunal assemblage has been collected from the Kilmaluag Formation of the Strathaird Peninsula, making it a globally significant locality for terrestrial Middle Jurassic fossil material (Pancioli *et al.* 2020b). The assemblage comprises hybodontiform sharks, amiiiform, pycnodontiform and semiodontiform actinopterygian fish, lissamphibians, testudines, lepidosaurs, choristoderes, archosaurs (including crocodylomorphs, dinosaurs and pterosaurs), mammaliamorphs, mammaliaforms and mammals (for an overview see Pancioli *et al.* 2020b and cites therein; also Jones *et al.* 2022; Tañanda *et al.* 2022; Pancioli *et al.* 2024). The composition of the vertebrate fossil assemblage is similar to that of the Forest Marble Formation at Kirtlington Cement Quarry in southern England, with many of the same taxa present (Pancioli *et al.* 2020b). Many taxa named from Kirtlington based on isolated skeletal elements and dentition were first collected in the Kilmaluag Formation, but not studied at the time of their original collection, instead remaining in the collections at the University of Bristol and National Museums Scotland.

Fossil material from the Kilmaluag Formation includes substantially more complete skeletons than those found at other Middle Jurassic localities in the UK, most notably Kirtlington Cement Quarry. This is partly due to different preservational environments, and also different collection methods. Kirtlington represents a brackish to marine estuarine environment (Barron *et al.* 2012), and material was bulk processed using screenwashing (e.g., Freeman 1979). Specimens from the Kilmaluag are located by eye, removed using rock-cutting equipment, and micro-CT or synchrotron scanning is used to study their anatomy, in contrast to being recovered by bulk sampling, as is common at coeval sites in the rest of the UK and Europe (Pancioli *et al.* 2020b).

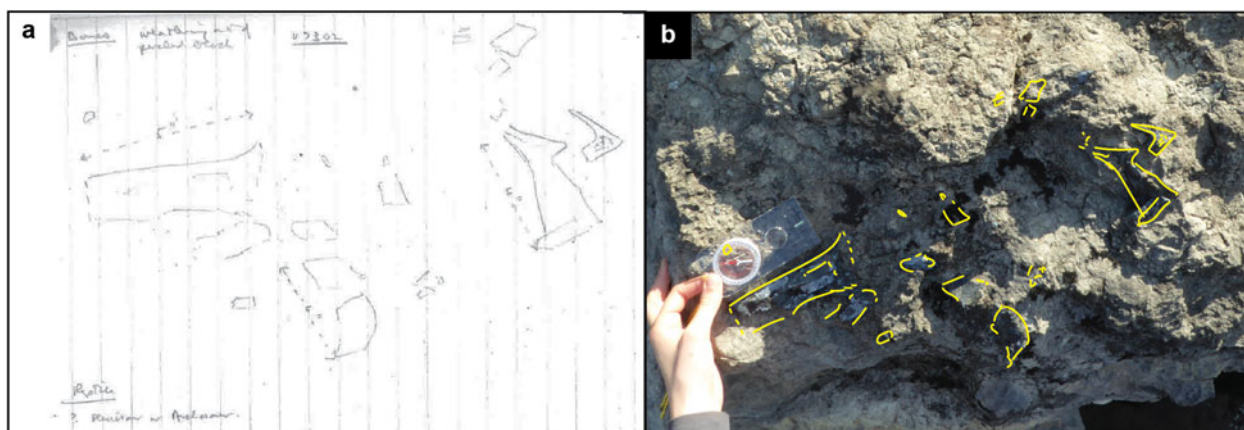


Figure 2 Initial discovery of NMS G.2023.19.1: (a) field notebook of Professor Savage showing specimen and notes made in 1973; (b) *in situ* fossil, photographed in 2016, with Savage's sketch overlaid in yellow.

The boulder containing NMS G.2023.19.1 is principally limestone and lacks distinctive bedding. Vertebrate bone fragments are concentrated in a restricted area confined to a single surface. The boulder has been dislodged from the cliff, but corresponds to beds 9b–i of the ‘Vertebrate Beds’ (Andrews 1985; Panciroli *et al.* 2020b).

3. Materials and methods

3.1. Extraction

The Elgol coastline has been given legal protection as a Site of Special Scientific Interest (SSSI), and through Scotland’s Nature Conservancy Order (NCO). Fossils can only be collected for

scientific purposes and require permits from NatureScot – these were obtained for this research.

The bones that comprise NMS G.2023.19.1 were exposed on the edge of a large protruding section of bedrock (boulder approximately $5 \times 2 \times 3$ m) just south of the Carn Mor landslip on the Strathaird Peninsula (Fig. 1c, d). The section was separated from the rest of the cliff by an eroded igneous dyke, and sat on the foreshore just above the highest tide line.

A block containing NMS G.2023.19.1 was extracted in April 2018 with technical expertise from Research Casting International (authors BLC and MF). The block was detached from the parent rock using traditional plug-and-feather stone-quarrying techniques, and lowered to beach level using slings



Figure 3 The process of extracting the dinosaur-bearing block: (a) the area of interest was supported by expanding eye bolts attached to a static anchor by slings, and a series of 25 mm diameter holes were drilled around this area; (b), plug-and-feather steel expanding wedges were inserted into the drill holes and struck with hammers in order to propagate cracks that separated the block from the rest of the pinnacle; (c–e) the detached block was lowered to the next level using a ratchet winch, and guided onto a board on a ramp constructed from 100 mm fencing posts onto the limestone pavement beneath; (f) the block was then secured to a wooden cradle by ratchet straps and carried over the beach to be loaded onto a rigid inflatable dinghy, which was towed (g) through Loch Scavaig to the landing jetty at Elgol; (h) the excavation team, from left to right: Roger Close, Brett Crawford, Stig Walsh (top), Andrzej Wolniewicz (bottom), Matt Fair, Elsa Panciroli, Richard Butler and Roger Benson. Photographs a–g by Elsa Panciroli.

anchored into the block and controlled by a mechanical ratchet (Fig. 3a–e). The block was transported from the extraction site to a landing site in the village of Elgol in a semi-rigid inflatable boat towed by a motor boat (Fig. 3f–h).

3.2. Manual preparation and digital imaging

Fine-chisel mechanical preparation was carried out by Scott Moore-Fay, augmented by localised application of cloths soaked with 10% formic acid on areas of prepared matrix to improve visual contrast between matrix and fossil bone. However, few diagnostic features were revealed in the exposed fossil bone fragments.

The prepared block was broken into four main fragments by RBJB to facilitate X-ray micro-CT scanning. Three smaller fragments were also created but not scanned. All seven fragments are numbered NMS G.2023.19.1.1–7 for precise part identification (see Fig. 4). Two thin sections were made from NMS G.2023.19.1.1 and are numbered NMS G.2023.19.1.8 and 9 (Fig. 4). Initial micro-CT data acquisition was carried out at the Natural History Museum using a Nikon XT H 225 ST system, and later at the University of Warwick using a Nikon XT H 450 RT, but the size of the blocks and the composition of the muddy micritic matrix meant the data obtained did not produce informative segmentations. Further scans were completed at the μ -VIS X-ray Imaging Centre of the University of Southampton (ESPRC grant EP/T02593X/1) using a diondo D5 system with a 450 kV mini-focus source. The scan parameters for

each part of the specimen are outlined in Table 1. Digital reconstruction was completed by EP using Materialise Mimics 19.0. Micro-CT scanning provided only limited additional information on bone morphology due to lack of contrast between the bones and matrix (Fig. 5). Consequently, the description is based primarily on observations of the bones lying *in situ* on the surface of the boulder, with measurements taken using callipers.

A photogrammetric model of NMS G.2023.19.1 was created by Matt Humpage (Northern Rogue Studios) after reduction of the specimen for micro-CT scanning. The model was made using 50 still TIFFs taken using a Nikon D3500 DSLR, and the point clouds and final model were made using 3DF Zephyr. The photogrammetric model is available on Sketchfab <https://sketchfab.com/3d-models/elgol-dinosaur-model-e773c97044ee4919b8d50517a2ab14c0>, and micro-CT data and PLYs are free to download at MorphoSource www.morphosource.org/projects/000700944?locale=en.

3.3. Palaeohistology

Palaeohistological thin sections were made by GFF following a modified petrographic sectioning procedure (Lamm 2013). A portion of bone (probably rib) was removed from NMS G.2023.19.1.1 using a Dremel rotary saw, and embedded in Buehler Epothin II epoxy resin under a vacuum (–25 inHg). The block was left to cure overnight, and was then cut at the

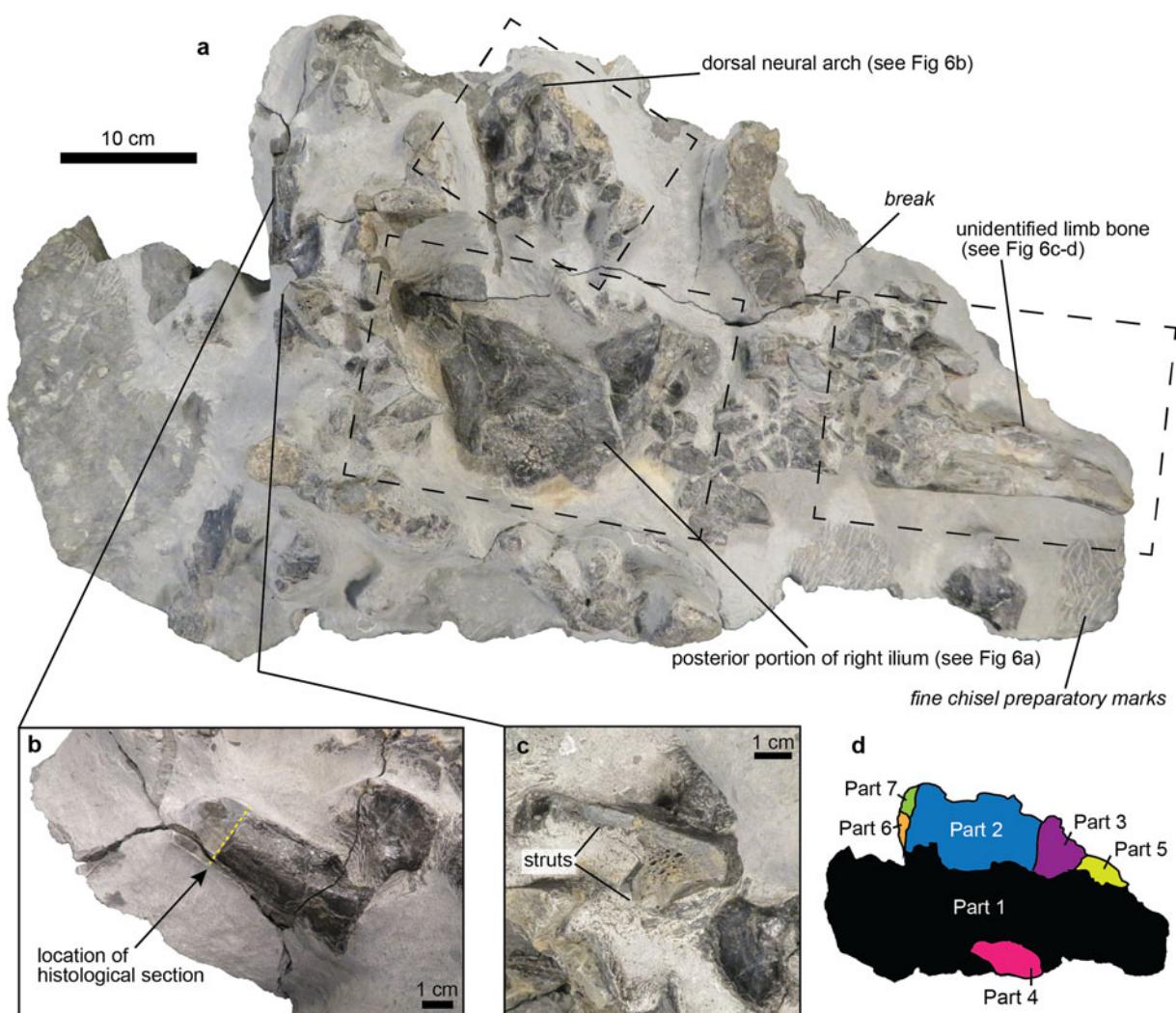


Figure 4 Overview of NMS G.2023.19.1.1–7: (a) whole specimen with all parts; (b) location of histological section, indicated by dotted yellow line; (c) fragment of dorsal rib exposed in cross-section; (d) schematic overview of parts 1–7 of NMS G.2023.19.1.

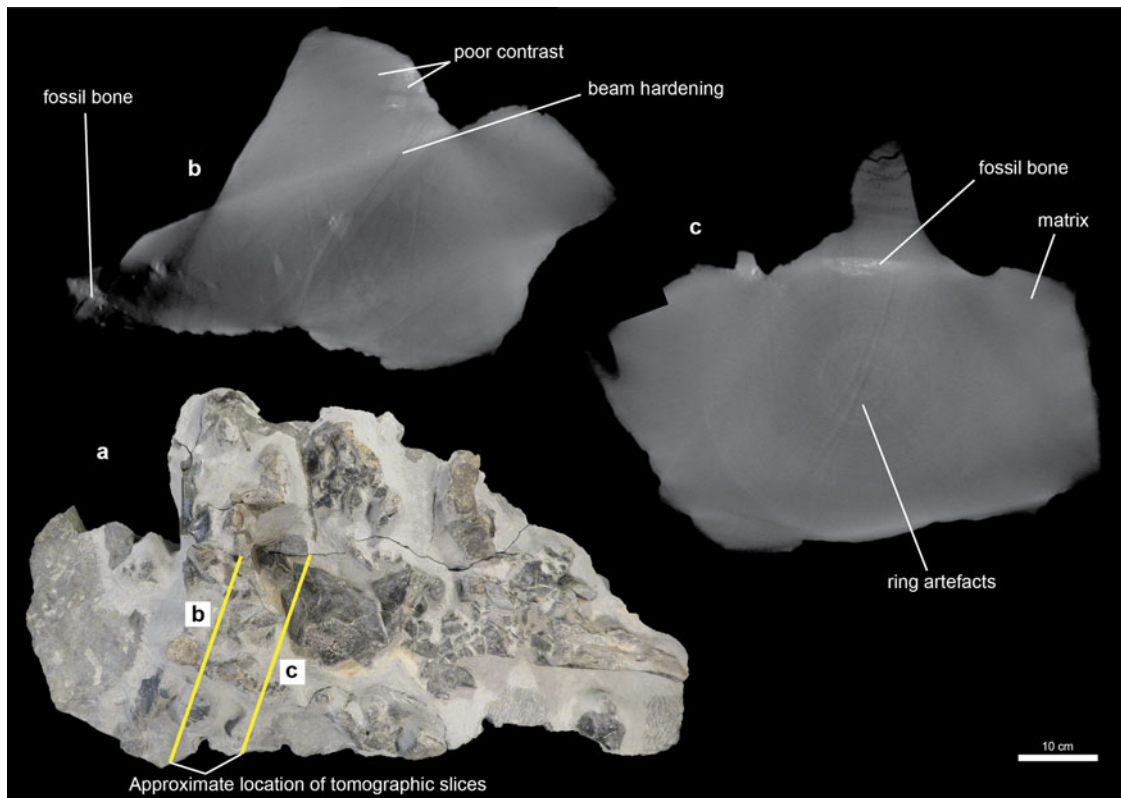


Figure 5 Samples of micro-CT data showing poor contrast and artefacts: (a) whole specimen indicating approximate locations of tomographic slices in (b) and (c) marked with yellow lines; (b) and (c) tomographic slices showing poor contrast and artefacts due to large sample size and density of limestone.

Table 1 Micro-CT scan parameters

Specimen	Detector	Resolution (μm)	kV	μA	Filter
NMS G.2023.19.1.1	3 K diondo 4343 HE Flat panel detector	219	440	3250	1.2 Cu
NMS G.2023.19.1.2	Perkin Elmer XRD 1621 CN14 HS detector	215	420	387	no filter
NMS G.2023.19.1.3	3 K diondo 4343 HE Flat panel detector	107	440	1050	0.6 Cu filter
NMS G.2023.19.1.4	3 K diondo 4343 HE Flat panel detector	107	440	1050	0.6 Cu filter

plane of interest using a Buehler Isomet 1000 Precision Saw with a Buehler 15LC wafering blade.

The part and counterpart of the cut billet, and a Plexiglas slide for each, were frosted on a glass plate using 600-grit silicon carbide abrasive slurry, to improve adhesion during mounting. Each billet was mounted to the frosted slide using Mercury M5 T cyanoacrylate adhesive and left to cure for at least 2 h. The mounted billets were re-sectioned using the Isomet 1000 saw to a thickness of 0.7 mm, and were then ground using a Hillquist Thin Section Machine until it neared the desired thickness ($\sim 100 \mu\text{m}$). Thereafter, they were ground to their final thickness (30–50 μm) using 600-grit silicon carbide abrasive slurry on a glass plate.

Upon grinding, it was discovered that the vacuum pressure during epoxy embedding was not sufficient to allow epoxy to penetrate deeply into the specimen, and some areas became powdery and were lost once they approached the target thickness. To mitigate this, the part slide was ground to a thickness that minimised damage to these powdery regions, whereas the counterpart slide was ground thinner, to maximise clarity of histological features regardless of damage. The slides (NMS G.2023.19.1.8–9) underwent a final polish using 1 μm aluminium oxide slurry.

Slides were observed under high magnification using a Nikon Eclipse microscope under plane-polarised and cross-polarised light (with and without a λ -filter) to identify bone matrix types based on osteocyte lacunae characteristics and polarisation

extinction patterns (following Padian & Lamm 2013 and de Buffrénil *et al.* 2021). Slides were then imaged under plane-polarised light using a lower-magnification Nikon AZ-100 microscope with a motorised Prior Stage and DS-Fii camera, using NIS Elements BR software, which allowed the entire slide to be imaged as a photomosaic.

4. Results

4.1. Description

The specimen consists of numerous bones and bone fragments that appear to be associated and lying on a single bedding plane within an area of approximately 60 cm by 40 cm. It is not possible to estimate the total number of bones. The matrix in which the bones are lying comprises hard limestone, precluding complete extraction.

All of the bones are broken and the external surfaces are extremely fractured. It is difficult to positively identify any single bone or anatomical details. Some individual pieces of bone are substantial in size, in the order of 15 to 20 cm in maximum dimensions as preserved. Given the poor preservation, only those elements that can be tentatively identified are described.

A possible dorsal neural arch is preserved in left lateral view on the surface of NMS G.2023.19.1.3 (Figs 4a, 6b). The centrum and neural spine, as well as the left transverse process, are not preserved. The left prezygapophysis, visible in lateral view,

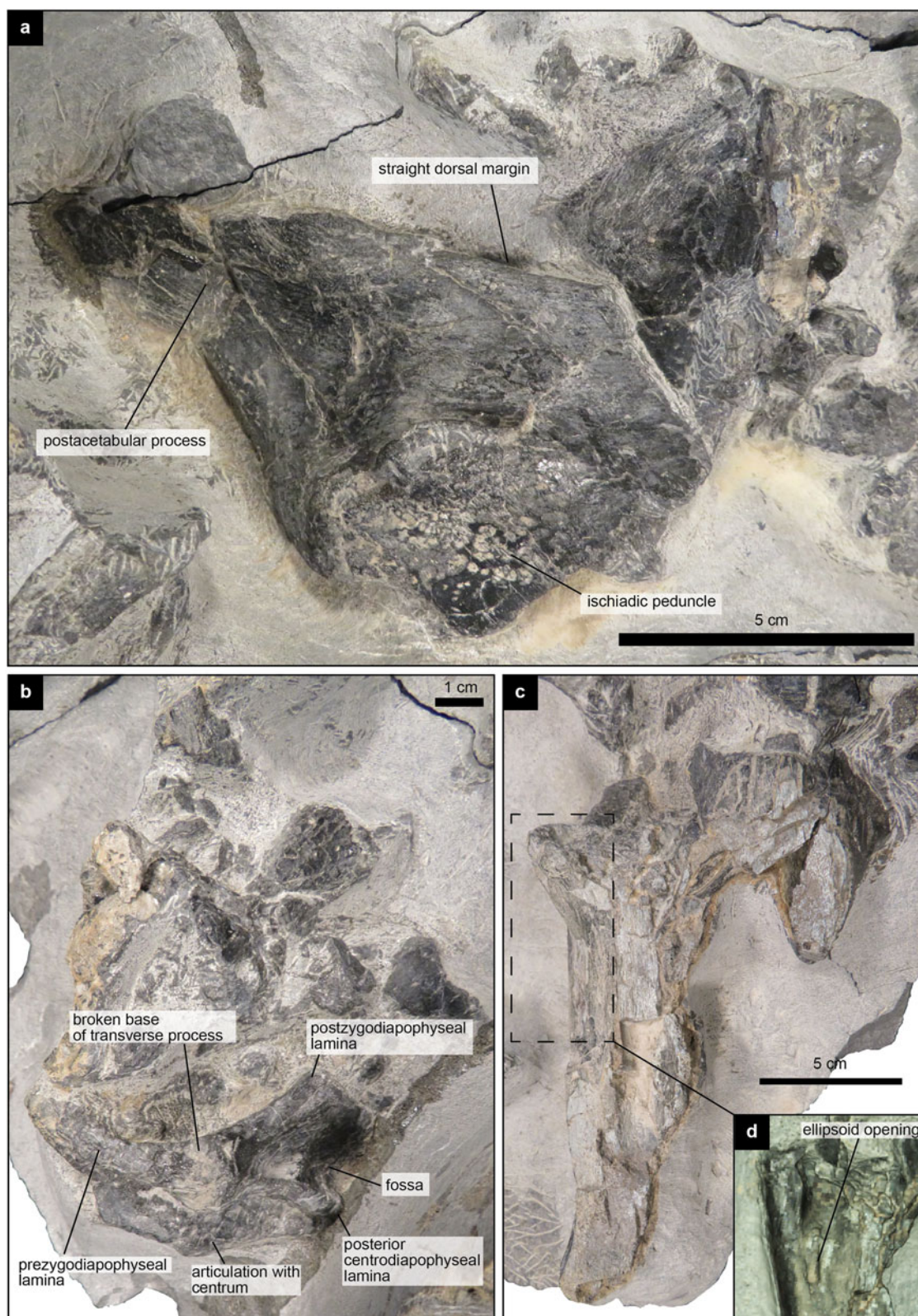


Figure 6 Close views of elements of NMS G.2023.19.1.1 and NMS G.2023.19.1.2: (a) NMS G.2023.19.1.1, posterior portion of a right ilium in lateral view; (b) NMS G.2023.19.1.2, dorsal neural arch is preserved in left lateral view; (c) NMS G.2023.19.1.1, elongate bone, possibly representing a limb element; (d) digital image of the elongate bone, taken from 3D model in slightly different orientation, clearly showing the ellipsoid opening.

extends anteriorly and is roughly triangular with an anterior apex and gently convex dorsal and ventral margins. The lateral surface of the prezygapophysis is gently convex and extends to the base of the broken transverse process in the form of a subtle prezygodiapophyseal lamina. Two further, better developed, laminae extend posteriorly from the base of the transverse process. The postzygodiapophyseal lamina extends posterodorsally, while the posterior

centrodiapophyseal lamina extends posteroventrally. Both are broken distally and form the margins of a fossa which would have formed the posterior part of the lateral surface of the neural arch. Ventral to the broken base of the transverse process, the lateral surface of the neural arch is gently concave.

A fragment of dorsal rib is exposed in cross-section on NMS G.2023.19.1.1 (Fig. 4c). It comprises two struts intersecting at

an acute angle. The strut that forms the dorsal surface of the rib is anteroposteriorly broad and dorsoventrally compressed. The second strut extends ventrally and slightly posteriorly and is anteroposteriorly broader than the dorsal strut. The margins of the struts merge gently with one another. The dorsal strut is composed of dense cortical bone, while the ventral strut is composed primarily of trabecular bone, except at its margins.

A large (~18 cm long) piece of bone, preserved close to the middle of the bone accumulation in NMS G.2023.19.1.1, possibly represents the posterior portion of a right ilium in lateral view (Figs 4a, 6a). The element is roughly triangular

as preserved with the apex pointing posteriorly; this apex represents the posterior margin of the postacetabular process. The ilium is transversely compressed with a straight dorsal margin that is not transversely expanded. Extending anteriorly from the posterior apex, the ventral margin of the postacetabular process slopes anteroventrally and terminates in an area with a pitted surface texture that appears to represent part of the ischiadic peduncle. This pitted surface is bounded by an anterodorsally curving ridge, fading anteriorly, that would have marked the posterior and dorsal margins of the ischiadic peduncle.

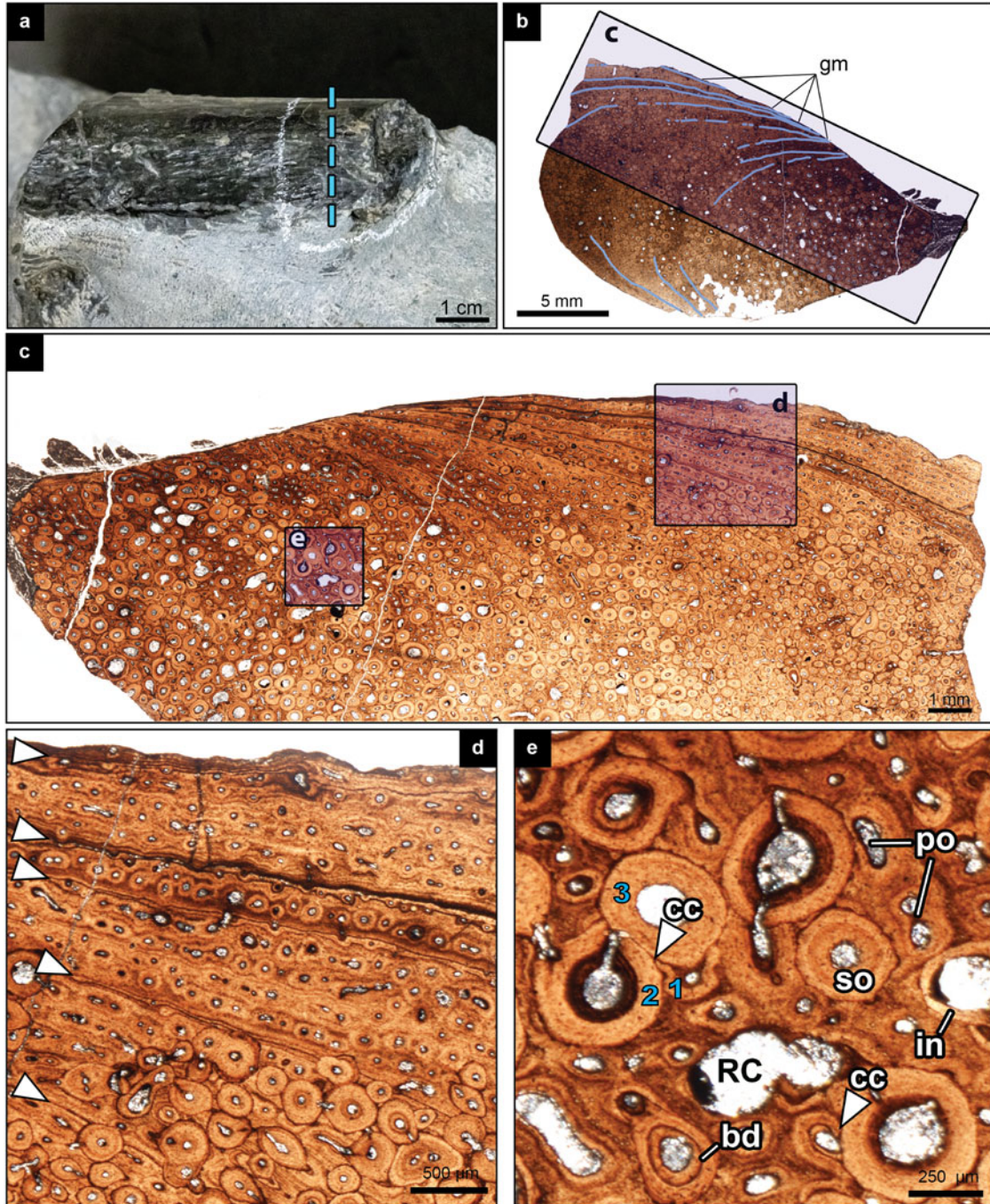


Figure 7 Osteohistology of NMS G.2023.19.1.8: (a) photograph of sampled element from NMS G.2023.19.1.1, with chalk outline showing the area removed by the Dremel for sampling, and dashed line showing the location of the thin sections; (b) overview image of entire sample NMS G.2023.19.1.8, with cyclical growth marks (gm) highlighted, and box showing the location of image (c); (c) photomontage of cortical region from counterpart section, showing porosity, secondary remodelling, cyclical growth marks and overall histological texture of the sample; (d) detail of cyclical growth marks (arrows) in the outer cortex of the sample; note multiple lines of arrested growth (LAGs) in some of the cyclical growth marks; (e) close-up of secondary remodelling and erosive cavities in the inner cortex; note cross-cutting relationships of secondary osteons, variation in secondary osteon infill and larger diameter of secondary osteons compared to primary osteons; numbers refer to three generations of cross-cutting secondary osteons. Scale bars as indicated. Abbreviations: bd = banding; cc = cross-cutting; gm = growth marks; in = incipient infill; po = primary osteon; RC = resorption cavity; so = secondary osteon.

Also preserved is an elongate bone (~20 cm long) (Figs 4a, 6c) with a large ellipsoid opening on its surface on NMS G.2023.19.1.1 (Fig. 6d). This opening may be a genuine anatomical feature or could have been taphonomically derived. This element appears to be a fragment of a limb bone, although further identification is not possible.

4.2. Histological description

A fragment of rib was selected for histological analysis based on ease of removal from the matrix, and confidence in identification of the element (Fig. 4b). The transverse thin sections (Fig. 7) show that the sampled bone was extensively eroded before preservation. Most of the sampled area comprises the outer cortex, and in some areas there is delamination at growth marks where periosteal bone has been lost. Towards the bottom of the slide (upwards as preserved in the field), histological structures are cross-cut at the surface, indicating that some of the bone in this area was eroded. The portion of the inner cortex that is preserved was probably adjacent or close to the medullary cavity in life, as it hosts some large resorption cavities and extensive secondary remodelling (Fig. 7e). However, the medullary cavity itself, if one was present in this element, is not preserved.

Primary bone throughout the sample consists of a woven-parallel (=fibrolamellar) complex with relatively dense longitudinal vascularity (Fig. 7c). Towards the periosteal surface in some regions, vasculature becomes less dense and the proportion of lamellar matrix increases, although the predominant longitudinal orientation of the vasculature is maintained. Osteocyte lacunae are present throughout the bone matrix; they are denser in the woven matrix than the lamellar matrix, but overall their preservation is relatively poor and they are difficult to discern or count.

Cyclical growth marks are present in the primary bone and can be traced around the cortex where they are not overprinted by secondary remodelling (Fig. 7b). At least eight cyclical growth marks can be discerned, although it is likely that more were present in the endosteal part of the cortex where remodelling is highest. It is also likely that cyclical growth marks have been lost from the periosteal surface, as delamination at the growth marks seems to have occurred in several places. Each of the cyclical growth marks comprises well-developed lines of arrested growth (LAGs), and many of the growth marks manifest double, triple or even quadruple LAGs (Fig. 7d). The cyclical growth marks do not perfectly follow the periosteal margin, and towards the top and bottom of the specimen (down and up in the field, respectively), they merge towards the periosteal surface and crop out at an angle on the surface (Fig. 7c). This indicates active cortical drift over the course of growth, with greater deposition of bone towards the sides of the sample than the top and bottom (corresponding anatomical orientations cannot be discerned). However, even taking these differences into account, there is no evidence of substantial changes in growth mark spacing throughout the cortex, although the spacing between the second to fourth growth marks is larger than the other growth zones. Despite lower vascularity and a higher proportion of lamellar bone matrix, growth marks are not densely packed at the periosteal surface and there is not a well-developed external fundamental system (Fig. 7d). A small area at the periosteal surface in one region of the bone appears to exhibit more closely packed LAGs, but it is unclear whether this is a multi-LAG growth mark that has lost more surficial bone, or if it results from growth dynamics related to cortical drift. Nevertheless, as this area does not extend far along the surface, it is clear that it does not constitute an external fundamental system.

Secondary remodelling is present throughout a substantial portion of the cortex (Fig. 7c), reaching the periosteal surface in some areas, but, where growth marks are most widely spaced,

it is absent after the sixth cyclical growth mark. The inner cortex is heavily remodelled by secondary osteons, but some primary bone remains in the interstitial spaces. Secondary osteons range in development: some have incipiently developed circumferential lamellae, whereas others have thick lamellae which occasionally show internal banding (Fig. 7e). The diameters of the secondary osteons are much greater than the primary osteons, and there is a general trend of decreasing secondary osteon size from the inner cortex towards the periosteal surface (Fig. 7c). In most areas only a single generation of secondary osteons can be discerned, with small regions of interstitial primary bone, but, especially towards the inner cortex, there are cross-cutting relationships indicating multiple generations of remodelling (Fig. 7e). At most, three generations of cross-cutting secondary osteons can be observed in the sample.

5. Discussion

5.1. Taxonomic affinities

Given the Middle Jurassic age of the specimen and the size of the individual bones, the specimen probably pertains to either a marine reptile or a dinosaur. The woven-parallel bone matrix with dense vasculature is indicative of relatively fast growth (Lee *et al.* 2013), although the longitudinal vasculature throughout the cortex suggests that this particular element was growing on the slow end of this spectrum (Castanet *et al.* 2000; de Margerie *et al.* 2002). Woven-parallel bone matrices are also present in some contemporary marine reptiles, particularly ichthyosaurs and plesiosaurs (de Buffr enil *et al.* 2021), but NMS G.2023.19.1 lacks characteristic histological features present in those groups. Specifically, the cortex does not show any evidence of adaptation for an aquatic lifestyle, either through osteoporosis (increased bone resorption and porosity) or pachyostosis (reduced bone porosity) (Houssaye 2009; Houssaye *et al.* 2014; Wintrich *et al.* 2017). Instead, the cortical porosity and evidence of small resorption cavities are similar to those described in terrestrial tetrapods including dinosaurs (Redelstorff & Sander 2009; Sander *et al.* 2011; Woodward *et al.* 2015; Panciroli *et al.* 2020a).

Furthermore, NMS G.2023.19.1 does not show the abundant radial vasculature described as 'plesiosaur radial bone', a common feature of plesiosaurs (Wintrich *et al.* 2017; de Buffr enil *et al.* 2021). Instead, the longitudinal vasculature and well-developed growth marks differ from the typical bone microstructure of plesiosaurs. Thalattosuchian crocodylians do exhibit cyclical growth marks like those in NMS G.2023.19.1, but even the largest teleosaurids exhibit predominantly lamellar or parallel-fibred bone matrices (de Buffr enil *et al.* 2021), not the well-developed woven-parallel bone matrix present throughout the cortex of NMS G.2023.19.1. Thus, the bone microstructure of NMS G.2023.19.1 differs fundamentally from those of contemporary large-bodied marine animals, but it is entirely within the range of variation for a dinosaur.

Due to the highly fragmentary state of preservation of the specimen, further determination of the affinities of the specimen is difficult and must be considered tentative. The microstructure of NMS G.2023.19.1 is reminiscent of a contemporary Scottish dinosaur from the nearby Isle of Eigg (Panciroli *et al.* 2020a). Both specimens show a woven-parallel bone matrix with well-developed cyclical growth marks and high rates of remodelling (Fig. 7). Neither shows evidence of an open medullary cavity, as would be expected of a theropod, and so in general they are more consistent with an ornithischian or sauropod identity.

Given the age of the specimen, the relatively simple structure of the neural arch, if correctly identified, tends to favour an interpretation of ornithischian affinities. By the Middle Jurassic, sauropods had evolved extensive pneumaticity of the axial skeleton,

and their vertebrae tend to be characterised by a network of well-developed and extensive laminae (e.g., Wedel 2003; Yates *et al.* 2012). In contrast, laminae in ornithischian dinosaurs are much more simple and generally poorly developed. In particular, the bifurcating postzygodiapophysial and posterior centrodiapophysial laminae identified on the neural arch of NMS G.2023.19.1 are reminiscent of those on some contemporary stegosaurs (e.g., *Stegosauria* indet. OUMNH J69710; *Adraklit*, Maidment *et al.* 2020) and some later ornithopods (e.g., *Tenontosaurus*, Forster 1990; *Camptosaurus*, Carpenter & Galton 2018; *Cummor*, Maidment *et al.* 2023). Eurypodan thyreophorans (stegosaurs and ankylosaurs) are characterised by the possession of ribs with a 'T'-shaped cross-section (Vickaryous *et al.* 2004; Maidment *et al.* 2021), although this is not always fully developed in the distal parts of the rib shafts. The lack of a 'T'-shaped cross-section in NMS G.2023.19.1 could be interpreted to suggest that this specimen is not a eurypodan thyreophoran.

If correctly identified, the transversely compressed morphology of the ilium is also inconsistent with a thyreophoran identification for the specimen, because the ilia of all except the most basal thyreophorans (which tend to be smaller than this specimen, e.g., *Scutellosaurus*; Breeden *et al.* 2021) are transversely expanded along the dorsal margin. Conversely, the ilia of early-diverging neornithischians, cerapodans and non-hadrosauriform ornithopods are transversely compressed (Butler *et al.* 2008). Notably, the pitted surface texture of the feature identified here as the ischiadic peduncle and the ridge extending around its margin are both observed in the early-diverging iguanodontian *Cummor* from the Late Jurassic of the UK (Maidment *et al.* 2023). Although the highly fragmentary state of NMS G.2023.19.1 precludes definitive identification, we suggest that the specimen represents a basal cerapodan or ornithopod, and perhaps even an iguanodontian, given its size and similarity to *Cummor*.

The oldest definitive ornithopod is the iguanodontian *Callovosaurus leedsii*, a femur from the Callovian Oxford Clay Formation of the UK (Ruiz-Omeñaca *et al.* 2007). However, relatively large tridactyl footprints attributed to ornithopods (probably iguanodontians) are known from other Bathonian localities in the UK and Morocco (Romano & Whyte 2003; Klein *et al.* 2023; Oussou *et al.* 2023), including Skye (Delair & Sarjeant 1985; dePolo *et al.* 2020), and indicate that iguanodontians had probably evolved by this time. It is possible that NMS G.2023.19.1.1–7 could represent the world's oldest ornithopod and perhaps even iguanodontian body fossil.

5.2. Ontogeny and growth

Osteohistological maturity signals (Lee *et al.* 2013) indicate that this individual was growing actively, but relatively slowly. The presence of at least eight cyclical growth marks indicates a minimum age of eight years (Köhler *et al.* 2012), but it is highly likely that more growth marks were present in the densely remodelled inner cortex, and have been lost from the delaminating periosteal surface. Growth marks are spaced relatively evenly, and there is no external fundamental system (Woodward *et al.* 2011) that would indicate a growth asymptote.

However, if substantial bone was indeed lost from the periosteal surface, it could have included the external fundamental system, making this assertion ambiguous. Nevertheless, vascular and bone matrix signals indicate a decrease in growth towards the end of life (Castanet *et al.* 2000; de Margerie *et al.* 2002; de Margerie 2004), suggesting that this was an individual that was probably nearing adult body size. Likewise, high rates of remodelling throughout the bone are consistent with somewhat advanced age, as remodelling tends to progress from the endosteal region towards the periosteum over the course of life (De Buffrénil & Quilhac 2021). Overall, the combination of growth

signals in NMS G.2023.19.1, as preserved, is most consistent with a subadult or young adult individual.

6. Conclusions

The Middle Jurassic of Scotland is increasingly well represented by the fossil discoveries from the Kilmaluag Formation, making it of global importance in our knowledge of this time period in tetrapod evolution. The partial skeleton NMS G.2023.19.1 is the first definite dinosaur body fossil discovered from Scotland, having been found in 1973, but not collected until 45 years later. It is also the most complete definite dinosaur known from Scotland, despite being broken into fragments, with a partial ilium, neural arch and portions of ribs and other pieces of larger elements.

If NMS G.2023.19.1 does represent an ornithischian, as tentatively suggested from the partial ilium and histological sectioning, it represents the geologically youngest known occurrence in Scotland, and first from the Kilmaluag Formation.

7. Acknowledgements

We would like to thank NatureScot and the John Muir Trust for permission to carry out fieldwork along the Elgol SSSI, and NatureScot for permits to collect this specimen. We are grateful to the generosity of Frederick Paulsen and Malcolm Offord for supporting specimen preparation and logistics for this project. Thanks go to our dedicated fieldwork team, including Andrzej Wolniewicz, Roger Close and Yves Candela. We are deeply indebted to Peter May from Research Casting International, and to the late Brett Crawford, for donating his time, expertise and strength to collecting this fossil from a logistically challenging location. We want to thank the crew of the *Bella Jane* – David, Doreen, Nick, Kristen and Donald – who fought wind and waves to get our specimen and crew from the site and back to shore. Thanks to Vincent Fernandez at the NHMUK, and teams at the University of Warwick (Guillaume Remy, Mark Williams and Paul Wilson) and University of Southampton (Fernando Alvarez Borges, Mark Mavrogordato, Erick Montes De Oca Valle, and Katy Rankin), for obtaining micro-CT data.

8. References

- Andrews, J. E. 1985. The sedimentary facies of a late Bathonian regressive episode: the Kilmaluag and Skudiburgh Formations of the Great Estuarine Group, Inner Hebrides, Scotland. *Journal of the Geological Society* **142**, 1119–37.
- Arkell, W. J. 1933. *The Jurassic System in Great Britain*. Oxford: Clarendon Press.
- Barrett, P. M. 2006. A sauropod dinosaur tooth from the Middle Jurassic of Skye, Scotland. *Earth and Environmental Science Transactions of the Royal Society of Edinburgh* **97**, 25–29.
- Barron, A. J. M., Lott, G. K. & Riding, J. B. 2012. Stratigraphic framework for the Middle Jurassic strata of Great Britain and the adjoining continental shelf: research report RR/11/06. British Geological Survey, Keyworth. 177 pp.
- Benson, R. B. J., Butler, R. J., Alroy, J., Mannion, P. D., Carrano, M. T. & Lloyd, G. T. 2016. Near-stasis in the long-term diversification of Mesozoic tetrapods. *PLoS Biology* **14**, e1002359.
- Benton, M. J., Martill, D. M. & Taylor, M. A. 1995. The first dinosaur from the Lower Jurassic of Scotland: a limb bone of a ceratosaur theropod. *Scottish Journal of Geology* **31**, 171–82.
- Breeden, B. T., Raven, T. J., Butler, R. J., Rowe, T. B. & Maidment, S. C. R. 2021. The anatomy and palaeobiology of the early armoured dinosaur *Scutellosaurus lawleri* (Ornithischia: Thyreophora) from the Kayenta Formation (Lower Jurassic) of Arizona. *Royal Society Open Science* **8**, 201676.
- Brusatte, S. L. & Clark, N. D. L. 2015. Theropod dinosaurs from the Middle Jurassic (Bajocian–Bathonian) of Skye, Scotland. *Scottish Journal of Geology* **51**, 157–64.

- Brusatte, S. L., Nesbitt, S. J., Irmis, R. B., Butler, R. J., Benton, M. J. & Norell, M. A. 2010. The origin and radiation of the dinosaurs. *Earth-Science Reviews* **101**, 68–100.
- Butler, R. J., Upchurch, P. & Norman, D. B. 2008. The phylogeny of the ornithischian dinosaurs. *Journal of Systematic Palaeontology* **6**, 1–40.
- Carpenter, K. & Galton, P. M. 2018. A photo documentation of bipedal ornithischian dinosaurs from the Upper Jurassic Morrison Formation, USA. *Geology of the Intermountain West* **5**, 167–207.
- Castanet, J., Rogers, K. C., Cubo, J. & Jacques-Boisard, J. 2000. Periosteal bone growth rates in extant ratites (ostrich and emu). Implications for assessing growth in dinosaurs. *Comptes Rendus de l'Académie des Sciences, Series III, Sciences de la Vie* **323**, 543–50.
- Clark, N. D. L. 2001. A thyreophoran dinosaur from the early Bajocian (Middle Jurassic) of the Isle of Skye, Scotland. *Scottish Journal of Geology* **37**, 19–26.
- Clark, N. D. L. 2018a. Hunting dinosaurs in the Middle Jurassic of Scotland. *Transactions of the Gaelic Society of Inverness* **69**, 59–77.
- Clark, N. D. L. 2018b. Review of the dinosaur remains from the Middle Jurassic of Scotland, UK. *Geosciences* **8**, 53.
- Clark, N. D. L., Boyd, J. D., Dixon, R. J. & Ross, D. A. 1995. The first Middle Jurassic dinosaur from Scotland: a cetiosaurid? (Sauropoda) from the Bathonian of the Isle of Skye. *Scottish Journal of Geology* **31**, 171–76.
- Clark, N. D. L. & Gavin, P. 2016. New Bathonian (Middle Jurassic) sauropod remains from the Valtos Formation, Isle of Skye, Scotland. *Scottish Journal of Geology* **51**, 71–75.
- Clark, N. D., Ross, D. A. & Booth, P. 2005. Dinosaur tracks from the Kilmaluag Formation (Bathonian, Middle Jurassic) of Score Bay, Isle of Skye, Scotland, UK. *Ichnos* **12**(2), 93–104.
- Cohen, K. M., Harper, D. A. T., Gibbard, P. L. & Fan, J.-X. 2019. *International chrono stratigraphic chart*. International Commission of Stratigraphy. <https://stratigraphy.org/chart>.
- de Buffrénil, V., de Ricqlès, A. J., Zylberberg, L. & Padian, K. (eds.) 2021. *Vertebrate skeletal histology and paleohistology*. Boca Raton: CRC Press.
- de Buffrénil, V. & Quilhac, A. 2021. Bone remodelling. In De Buffrénil, V., De Ricqlès, A., Zylberberg, L. & Padian, K. (eds) *Vertebrate skeletal histology and paleohistology*, 229–46, 1st ed. Boca Raton: CRC Press.
- Delair, J. B. & Sarjeant, W. A. S. 1985. History and bibliography of the study of fossil vertebrate footprints in the British Isles: supplement 1973–1983. *Palaeogeography Palaeoclimatology Palaeoecology* **49**, 123–60.
- de Margerie, E. 2004. Assessing a relationship between bone microstructure and growth rate: a fluorescent labelling study in the King Penguin chick (*Aptenodytes patagonicus*). *Journal of Experimental Biology* **207**, 869–79.
- de Margerie, E., Cubo, J. & Castanet, J. 2002. Bone typology and growth rate: testing and quantifying 'Amprino's rule' in the Mallard (*Anas platyrhynchos*). *Comptes Rendus Biologies* **325**, 221–30.
- dePolo, P. E., Brusatte, S. L., Challands, T. J., Foffa, D., Wilkinson, M., Clark, N. D. L., Hoad, J., Gomes da Costa Pereira, P. V. L., Ross, D. A. & Wade, T. J. 2020. Novel track morphotypes from new tracksites indicate increased Middle Jurassic dinosaur diversity on the Isle of Skye, Scotland. *PLoS ONE* **15**, e0229640.
- Ezcurra, M. D., Marke, D., Walsh, S. A. & Brusatte, S. L. 2023. A revision of the 'coelophysoid-grade' theropod specimen from the Lower Jurassic of the Isle of Skye (Scotland). *Scottish Journal of Geology* **59**. DOI:10.1144/sjg2023-012
- Forster, C. A. 1990. The postcranial skeleton of the ornithomimid dinosaur *Tenontosaurus tilletti*. *Journal of Vertebrate Paleontology* **10**, 273–94.
- Freeman, E. F. 1979. A Middle Jurassic mammal bed from Oxfordshire. *Palaeontology* **22**, 135–66.
- Harris, J. P. & Hudson, J. D. 1980. Lithostratigraphy of the Great Estuarine Group (Middle Jurassic), Inner Hebrides. *Scottish Journal of Geology* **16**, 231–50.
- Houssaye, A. 2009. 'Pachyostosis' in aquatic amniotes: a review. *Integrative Zoology* **4**, 325–40.
- Houssaye, A., Scheyer, T. M., Kolb, C., Fischer, V. & Sander, P. M. 2014. A new look at ichthyosaur long bone microanatomy and histology: implications for their adaptation to an aquatic life. *PLoS One* **9**(4), e95637.
- Jones, M. E. H., Benson, R. B. J., Skutschas, P., Hill, L., Panciroli, E., Schmitt, A. D., Walsh, S. & Evans, S. E. 2022. Middle Jurassic fossils document an early stage in salamander evolution. *Proceedings of the National Academy of Sciences* **119**, e2114100119.
- Judd, J. W. 1878. The secondary rocks of Scotland. Third paper. The strata of the western coasts and islands. *Quarterly Journal of the Geological Society of London* **34**, 660–743.
- Klein, H., Gierlinski, G. D., Saber, H., Lallensack, J. N., Lagnaoui, A., Hminna, A. & Charrière, A. 2023. Theropod and ornithischian dinosaur track assemblages from the Middle to ?Late Jurassic deposits of the Central High Atlas, Morocco. *Historical Biology* **35**, 320–46.
- Köhler, M., Marín-Moratalla, N., Jordana, X. & Aanes, R. 2012. Seasonal bone growth and physiology in endotherms shed light on dinosaur physiology. *Nature* **487**, 358–61.
- Lamm, E.-T. 2013. Preparation and sectioning of specimens. In Padian, K. & Lamm, E.-T. (eds) *Bone histology of fossil tetrapods: advancing methods, analysis, and interpretation*, 55–160. Berkeley: University of California Press.
- Lee, A. H., Huttenlocker, A. K., Padian, K. & Woodward, H. N. 2013. Analysis of growth rates. In Padian, K. & Lamm, E.-T. (eds) *Bone histology of fossil tetrapods: advancing methods, analysis, and interpretation*, 217–252. Berkeley: University of California Press.
- Maidment, S. C. R., Chapelle, K. E. J., Bonsor, J. A., Button, D. & Barrett, P. M. 2023. Osteology and relationships of *Cummorja prestwichii* (Ornithischia: Ornithopoda) from the Late Jurassic of Oxfordshire, UK. *Monographs of the Paleontological Society* **176**, 1–55.
- Maidment, S. C. R., Raven, T. J., Ouarhache, D. & Barrett, P. M. 2020. North Africa's first stegosaur: implications for Gondwanan thyreophoran dinosaur diversity. *Gondwana Research* **77**, 82–97.
- Maidment, S. C. R., Strachan, S. J., Ouarhache, D., Scheyer, T. M., Brown, E. E., Fernandez, V., Johanson, Z., Raven, T. J. & Barrett, P. M. 2021. Bizarre dermal armour suggests the first African ankylosaur. *Nature Ecology & Evolution* **12**, 1576–81.
- Murchison, R. I. 1828. Supplementary remarks on the Strata of the oolitic series and the rocks associated with them in the Counties of Sutherland and Ross, and in the Hebrides. *Transactions of the Geological Society of London* **2**, 353–68.
- Oussou, A., Falkingham, P. L., Butler, R. J., Boumir, K., Ouarhache, D., Ech-charay, K., Charrière, A. & Maidment, S. C. R. 2023. New Middle to ?Late Jurassic dinosaur tracksites in the Central High Atlas Mountains, Morocco. *Royal Society Open Science* **10**, 231091.
- Peach, B. N. 1910. The geology of Glenelg, Lochalsh and south-east part of Skye. (Explanation of one-inch map 71.) Memoirs of the Geological Survey. H. M. Stationery Off., Morrison & Gibb.
- Padian, K. & Lamm, E.-T. (eds.) 2013. *Bone histology of fossil tetrapods: advancing methods, analysis, and interpretation*. Berkeley: University of California Press.
- Panciroli, E., Benson, R. B. J., Fernandez, V., Butler, R. J., Fraser, N. C., Luo, Z.-X. & Walsh, S. 2021. New species of mammaliaform and the cranium of *Borealestes* (Mammaliaformes: Docodonta) from the Middle Jurassic of the British Isles. *Zoological Journal of the Linnean Society* **192**, 1323–62.
- Panciroli, E., Benson, R. B. J., Fernandez, V., Fraser, N. C., Humpage, M., Newham, E., Walsh, S. & Luo, Z.-X. 2024. Jurassic fossil juvenile reveals prolonged life history in early mammals. *Nature* **632**, 815–22.
- Panciroli, E., Benson, R. B. J., Fernandez, V., Humpage, M., Martin-Serra, A., Walsh, S., Luo, Z.-X. & Fraser, N. C. 2022. Postcranial of *Borealestes* (Mammaliaformes, Docodonta) and the emergence of ecomorphological diversity in early mammals. *Palaeontology* **65**, e12577.
- Panciroli, E., Funston, G. F., Holwerda, F., Maidment, S. C. R., Foffa, D., Larkin, N., Challands, T., Depolo, P. E., Goldberg, D., Humpage, M., Ross, D., Wilkinson, M. & Brusatte, S. L. 2020a. First dinosaur from the Isle of Eigg (Valtos Sandstone Formation, Middle Jurassic), Scotland. *Earth and Environmental Science Transactions of the Royal Society of Edinburgh* **111**, 157–72.
- Panciroli, E., Benson, R. B., Walsh, S., Butler, R. J., Castro, T. A., Jones, M. E. & Evans, S. E. 2020b. Diverse vertebrate assemblage of the Kilmaluag Formation (Bathonian, Middle Jurassic) of Skye, Scotland. *Earth and Environmental Science Transactions of the Royal Society of Edinburgh* **111**, 135–56.
- Redelstorff, R. & Sander, P. M. 2009. Long and girdle bone histology of *Stegosaurus*: implications for growth and life history. *Journal of Vertebrate Paleontology* **29**, 1087–99.
- Romano, M. & Whyte, M. A. 2003. Jurassic dinosaur tracks and trackways of the Cleveland Basin, Yorkshire: preservation, diversity and distribution. *Proceedings of the Yorkshire Geological Society* **54**, 185–215.
- Ruiz-Omeñaca, J. I., Pereda Suberbiola, X. & Galton, P. M. 2007. *Callovosaurus leedsi*, the earliest dryosaurid dinosaur (Ornithischia: Euornithopoda) from the Middle Jurassic of England. In Carpenter, K. (ed.), *Horns and beaks: ceratopsian and ornithomimid dinosaurs*, 3–16. Bloomington: Indiana University Press.
- Sander, P. M., Klein, N., Stein, K. W. H. & Wings, O. 2011. Sauropod bone histology and its implications for sauropod biology. In Klein, N., Remes, K., Gee, C. & Sander, P. M. (eds) *Biology of the sauropod dinosaurs: understanding the life of giants*, 276–304. Bloomington: Indiana University Press.
- Talanda, M., Fernandez, V., Panciroli, E., Evans, S. E. & Benson, R. B. J. 2022. Synchrotron tomography of a stem lizard elucidates early squamate anatomy. *Nature* **611**, 99–104.

- Vickaryous, M. K., Maryńska, T. & Weishampel, D. B. 2004. Ankylosauria. In Weishampel, D. B., Dodson, P. & Osmólska, H. (eds) *The Dinosauria: second edition*, 363–92. Berkeley: University of California Press.
- Waldman, M. & Savage, R. J. G. 1972. The first Jurassic mammal from Scotland. *Journal of the Geological Society of London* **128**, 119–25.
- Wedel, M. J. 2003. The evolution of vertebral pneumaticity in sauropod dinosaurs. *Journal of Vertebrate Paleontology* **23**, 344–57.
- Whyte, S. & Ross, D. 2019. *Jurassic Skye: dinosaurs and other fossils of the Isle of Skye*. Berkshire, UK: NatureBureau.
- Wills, S., Barrett, P. M. & Walker, A. 2014. New dinosaur and crocodylomorph material from the Middle Jurassic (Bathonian) Kilmaluag Formation, Skye, Scotland. *Scottish Journal of Geology* **50**, 183–90.
- Wills, S., Underwood, C. J. & Barrett, P. M. 2021. Learning to see the wood for the trees: machine learning, decision trees, and the classification of isolated theropod teeth. *Palaeontology* **64**, 75–99.
- Wills, S., Underwood, C. J. & Barrett, P. M. 2023. Machine learning confirms new records of maniraptoran theropods in Middle Jurassic UK microvertebrate faunas. *Papers in Palaeontology* **9**, e1487.
- Wintrich, T., Hayashi, S., Houssaye, A., Nakajima, Y. & Sander, P. M. 2017. A Triassic plesiosaurian skeleton and bone histology inform on evolution of a unique body plan. *Science Advances* **3**, e1701144.
- Woodward, H. N., Freedman Fowler, J. E. A., Farlow, O. & Horner, J. R. 2015. *Maiaasaura*, a model organism for extinct vertebrate population biology: a large sample statistical assessment of growth dynamics and survivorship. *Paleobiology* **41**, 503–27.
- Woodward, H. N., Horner, J. R. & Farlow, J. O. 2011. Osteohistological evidence for determinate growth in the American alligator. *Journal of Herpetology* **45**, 339–42.
- Yates, A. M., Wedel, M. J. & Bonnan, M. F. 2012. The early evolution of postcranial skeletal pneumaticity in sauropodomorph dinosaurs. *Acta Palaeontologica Polonica* **57**, 85–100.
- Young, C. M. E., Hendrickx, C., Challands, T. J., Foffa, D., Ross, D. A., Butler, I. B. & Brusatte, S. L. 2019. New theropod dinosaur teeth from the Middle Jurassic of the Isle of Skye, Scotland. *Scottish Journal of Geology* **55**, 7–19.

MS received 5 September 2024. Accepted for publication 18 November 2024